

Flip Paths Between Lattice Triangulations

William Sims Meera Sitharam

Abstract

The problem of finding a diagonal *flip* path between two triangulations has been studied for nearly a century. In the geometric setting, finding a flip path between two triangulations containing the minimum number of flips is NP-complete. However, for minimum flip paths between lattice triangulations, Eppstein and Caputo et al. gave algorithms running in $O(n^2)$ time, where n is the number of points in the point-set. Eppstein proved this result for lattice point-sets bounded by convex polygons. Caputo et al. extended this result to the cases of non-convex bounding polygons and constrained flip paths that preserve a set of edges. In fact, Eppstein’s approach readily extends to both cases. Our first result shows that there is a unique, partially-ordered set of flips whose valid linear-orderings are exactly the constrained, minimum flip paths between two lattice triangulations, leading to an algorithm to compute such a minimum flip path in $O(n^{\frac{3}{2}})$ time. As a further improvement over previous results, in many natural cases, our algorithm runs in time linear in the length of the minimum flip path. Our second result characterizes pairs of triangulations T and T' that contain given sets of edges G and G' respectively, and attain the minimum flip path between each other, where the minimum is taken over such pairs of triangulations. Finally, we demonstrate how our results can model crack propagation in crystalline materials caused by Stone-Wales defects. Notably, the above results follow from simple number-theoretic and geometric concepts.

1 Introduction

Given a set of points S in \mathbf{R}^2 and a simple, closed polygonal region Ω with vertices in S , a *triangulation* of (S, Ω) is an embedding of a planar graph with vertex set $S \cap \Omega$, non-intersecting straight-line edges including the boundary edges of Ω , and triangular interior facets. Note that Ω need not be convex (see also Section 8). A triangulation can be transformed into another via a sequence of operations called *diagonal flips*, defined as follows.

Definition 1 (Diagonal Flip and Flip Path). *A diagonal flip (shortened to flip) is an operation transforming one triangulation T into another: for some convex quadrilateral in T whose interior contains only a diagonal edge, the flip operation replaces this diagonal edge with the other (Figure 1d). A flip path is a starting triangulation along with a sequence of flips (equivalently, the corresponding*

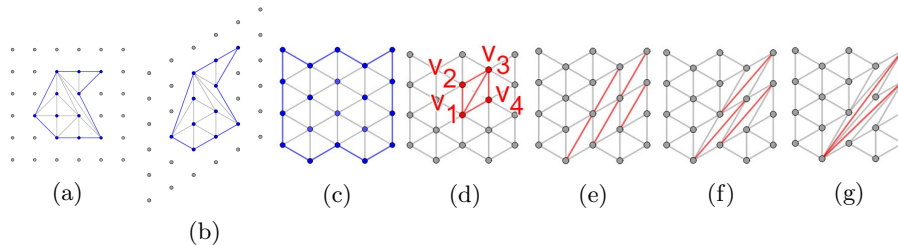


Figure 1: (a) is the integer lattice and a lattice triangulation bounded by a simple, closed polygon. (b) is an affine transformation of (a), yielding the triangular lattice and the transformed triangulation and bounding polygon. (c) - (g) show a flip path from the equilateral triangulation (Definition 4) in (c) to the triangulation in (g). (d) shows the first flip (Definition 1) along this flip path, performed on the red quadrilateral, which replaces the edge (v_2, v_4) with the edge (v_1, v_3) . The red edges in (e)-(g) result from flips in this flip path that may be performed simultaneously.

sequence of triangulations) ending with the target triangulation (Figures 1c - 1g).

Our results concern flip paths between *lattice triangulations* - i.e. triangulations of (L, Ω) , where L is an affine transformation of the integer lattice (Figures 1a and 1b). We sometimes refer to the *lattice point-set* $L \cap \Omega$ with *bounding polygon* Ω . We are interested in finding *minimum flip paths* between two lattice triangulations, i.e., with the minimum number of flips, taken over all flip paths between these triangulations.

1.1 Background and Motivation

For any set of points S and polygonal region Ω , the *flip graph* of (S, Ω) encodes flip paths between triangulations and is defined as follows: each vertex of the flip graph is a triangulation of (S, Ω) and each edge of the flip graph connects a pair of triangulations that differ by a single flip. The flip graph of (S, Ω) was first shown to be connected when Ω is a simple, closed, convex polygonal region, and the boundary vertices of Ω are exactly $S \cap \Omega$ - a result attributed to Lawson [13]. This result was then extended to any set of points S and simple, closed, but not necessarily convex polygonal regions Ω by Dyn et al. [7], who attribute the idea to Edelsbrunner. Their main proof technique was to give a *flip path that generates an edge* starting from a triangulation that does not contain that edge. More precisely, for any non-edge pair of vertices (u, v) in a triangulation T of (S, Ω) defining a line segment that contains only these two points, they showed how to find a flip path from T to *some* triangulation of (S, Ω) that contains the edge (u, v) . Osherovich et al. [18] gave alternative proofs of the previous two results using only simple geometric properties of polygons.

Although we are working exclusively in the Euclidean geometric setting, for

completeness, we point out that these flip graph connectivity questions also apply in the combinatorial setting, between triangulations of topological spaces - i.e. where a triangulation is embedded on a surface and the *topological flip* permits a homeomorphism of the surface. In this case, only the combinatorics, or graph, of the triangulation is relevant (the boundary facet is generally assumed to be a triangle). In fact, the combinatorial setting was explored nearly 40 years before the geometric setting. Flip graphs in the combinatorial setting were first shown to be connected when their vertices correspond to triangulations of small genus - e.g., that are embeddable (with non-crossing edges) on a sphere, torus, projective plane, or Klein bottle [26, 6, 17]. This result was generalized to triangulations of arbitrary closed surfaces [16] and later strengthened to the case of topological flips that only permit diffeomorphisms [15].

Returning to the geometric setting, our results concern the connectivity of flip graphs whose vertices are lattice triangulations. Lattice triangulations arise in algebraic geometry [3], discriminant theory [10], and quantum spin systems [2]; they are additionally connected to Hilbert's 16th problem [25]. Some work has gone into counting and enumerating lattice triangulations [2, 11, 12]. For a broad treatment of general and lattice triangulations, see [4].

1.1.1 Previous Work on Flip Paths Between Lattice Triangulations

In the geometric setting, the problem of finding a minimum flip path between two (not necessarily lattice) triangulations of (S, Ω) is NP-complete [1], for some point-set S and polygonal region Ω . However, when Ω is a convex polygonal region and the point-set $S \cap \Omega$ contains no empty, strictly convex pentagon, Eppstein [8] gave an algorithm for finding a minimum flip path between any two triangulations of (S, Ω) that runs in $O(n^2)$ time, where n is the number of points in $S \cap \Omega$. Lattice point-sets bounded by convex polygons have this non-empty-pentagon property. A few years later, Caputo et al. [2] gave an algorithm for finding a minimum flip path between any two lattice triangulations (whose bounding polygon need not be convex) that also runs in $O(n^2)$ time. In fact, this algorithm works for flip paths *constrained by* a set of edges E , i.e. where every triangulation in the flip path must contain a set of *constraint* edges E . While not stated, Eppstein's [8] result can be extended to handle non-convex bounding polygons and constrained flip paths. Also, both Eppstein [8] and Caputo et al. [2] proved that the set of flips in any minimum flip path between two lattice triangulations is unique. Although these results are stated for lattice triangulations coming from the integer lattice, the algorithms and proofs given carry over to affine transformations of this lattice, such as the triangular lattice. However, these algorithms do not consider the situation where only a target edge e is given. Our previous result [20] shows that there is a unique, partially-ordered set of flips whose valid linear-orderings are exactly the minimum flip paths between an equilateral lattice triangulation and a lattice triangulation containing e .

2 Contributions

Note on Terminology. From here on, all triangulations are lattice triangulations of (L, Ω) , for some fixed lattice L and polygonal region Ω . Our results rely only on the existence of *Farey* parallelograms (see Definition 7) in a triangulation, so they apply when L is any affine transformation of the integer lattice. Hence, without loss of generality, we let L be the triangular lattice; and when the context is clear, we omit mentioning (L, Ω) , and simply refer to “triangulations,” or occasionally to the *lattice point-set* $S = L \cap \Omega$ with bounding polygon Ω . The following are our main results.

1. We give an algorithm to compute a minimum flip path between two triangulations in $O\left(n^{\frac{3}{2}}\right)$ time, where n is the number of vertices in the lattice point-set S with bounding polygon Ω (Proposition 1), improving over the algorithms from Eppstein [8] and Caputo et al. [2] that take $O(n^2)$ time. Furthermore, in many input cases, our algorithm has linear output complexity, i.e., runs in time linear in the length of the output minimum flip path, a significant advantage over previous algorithms (Proposition 2). While Eppstein [8] and Caputo et al. [2] output a minimum flip path between two triangulations, and show that every minimum flip path between these triangulations contains the same set of flips, our structural result and algorithm explicitly give the partial order on this unique set of flips whose valid linear-orderings are exactly the set of minimum flip paths (Theorem 1).
2. We characterize pairs of triangulations T and T' that contain given sets of edges G and G' respectively, and attain the minimum flip path between each other, where the minimum is taken over all such pairs of triangulations. In contrast, previous algorithms require starting and target triangulations as input. This allows our algorithm to be used in scenarios where the input is only a set of long edges to be generated. Our previous result [20] considered the special case of generating a single target edge for the abovementioned modeling of crystalline crack propagation.
3. We demonstrate how to model the propagation of cracks in crystalline materials, such as silicon or graphene, caused by Stone-Wales defects using our results above. Additionally, we explore the limitations of this model and propose methods to improve it.

2.1 Basic Tools and Definitions

In this section, we present the concepts and tools necessary to formally state our results. First, we give a convenient way to represent an edge in a triangulation, or more generally, a line-segment between two lattice points.

Definition 2 (Edge and Edge Equivalence Class). An edge $e = (x, y)$ at a point v , is a vector (x, y) originating at a lattice point v , where x and y are nonnegative, relatively prime integer coefficients when the edge e is expressed as a linear combination of its defining coordinate pair of unit vectors (out of the 3 coordinate pairs) that minimize $|x| + |y|$.

An edge $e = (x, y)$ is the equivalence class under lattice shifts of the originating point v .

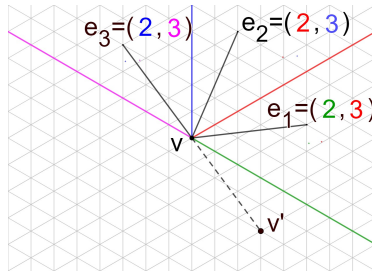


Figure 2: Three copies of the edge $(2, 3)$ with the same originating point v . For a given section of the plane, the ordering convention for an edge $(2, 3)$ is the anticlockwise ordering of the 2 relevant lattice unit vectors for that section, called the *defining coordinate pair* (see Section 2.1). Having specified the vector $(2, 3)$ and the lattice point v , we require 1 additional piece of information to uniquely specify an edge: the section of the plane that contains the edge. This information is encoded in the defining coordinate pair of an edge. Note, the dashed edge is in the same equivalence class as the edge e_3 and originates at the point v' .

See Figure 2 for examples of edges at points and an edge equivalence class. Throughout this paper, the additional piece of information that disambiguates the three edges with the same vector and originating point is always clear from the context, and is never explicitly specified or used. A default representative of the edge class $e = (x, y)$ that is commonly used is the edge (x, y) at the point $(0, 0)$. When we refer to an edge without specifying an originating point, it will be clear from the context whether we are referring to the edge equivalence class or to a default representative of this class.

When the starting triangulation is clear from the context, we shorten the expression a “flip path that generates a target edge at a point” to a *flip path for an edge at a point*. Note that the edge equivalence class induces a corresponding equivalence class of *flip paths for an edge*. We want to find a *minimum* flip path for an edge, i.e. containing the minimum number of flips.

The key structure of interest introduced in our previous paper [20] is the following.

Definition 3 (Flip Plan for a Single Edge). A flip plan that generates an edge e at the point v from a triangulation T , denoted by $\pi_{e,v}(T)$, is a partially-ordered

set of flips, whose valid linear-orderings are exactly the flip paths for the edge containing this set of flips.

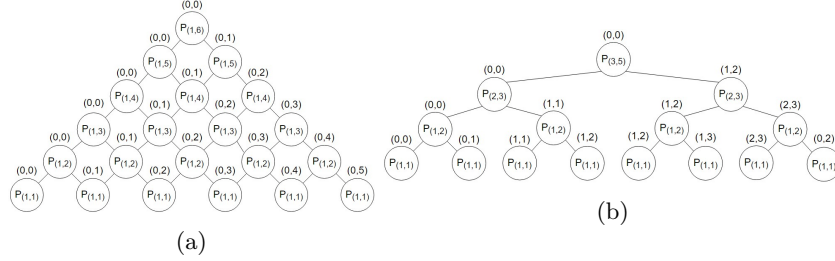


Figure 3: (a) and (b) show the minimum flip plans that generate the edges (1, 6) and (3, 5) from an equilateral triangulation (see Definition 4). The nodes are (flips performed on) Farey parallelograms (see Definition 7).

A flip plan is presented as a directed acyclic graph (DAG), because then we may refer to a flip's parent or child flips. The edges in a flip plan are always directed towards parent flips, so they are generally not shown. See Figure 3 for examples.

Now we introduce some convenient notation for working with flip plans. When the starting triangulation is clear from context, we refer to a *flip plan for an edge e at a point v* , denoted by $\pi_{e,v}$. The edge equivalence class induces an equivalence class of *flip plans for the edge e* , denoted by π_e . We are interested in finding the *minimum* flip plan for an edge. This is the flip plan whose valid linear-orderings are exactly the minimum flip paths for the edge. We prove this flip plan is unique in Section 3. We can easily extend this definition to talk about a flip plan that generates a set of edges $E = \{e_1, \dots, e_n\}$ at a set of points $V = \{v_1, \dots, v_n\}$ from a triangulation T , denoted by $\pi_{E,V}(T)$ - i.e. this flip plan generates e_1 at v_1 , e_2 at v_2 , and so on. Similarly, we obtain an equivalence class of flip plans for the edges in E , denoted by π_E . A default representative of this class places one edge in E at the point $(0,0)$.

Next, consider the flip plans $\pi_{e_1,u}$ and $\pi_{e_2,v}$ for the edge e_1 at the point u and the edge e_2 at the point v . Let $\pi_{e_1,u} \parallel \pi_{e_2,v}$ denote the unique partial order such that the only relationships between these flip plans are that the maximal flip in $\pi_{e_1,u}$ is a child of each leaf flip in $\pi_{e_2,v}$ - i.e., the edge e_1 at the point v must be generated before the edge e_2 at the point u . Also, let $\pi_{e_1,u} \cup \pi_{e_2,v}$ denote the unique partial order such that the flips in $\pi_{e_1,u}$ can be performed independently of the flips in $\pi_{e_2,v}$, and vice versa - i.e., the root flip in each flip plan is a maximal element in the partial order. The edge equivalence class induces equivalence classes of partial orders $\pi_{e_1} \parallel \pi_{e_2}$ and $\pi_{e_1} \cup \pi_{e_2}$. Common representatives of these classes place one edge at the point $(0,0)$.

A flip plan may also be defined between two triangulations T and T' analogously to the above definition. We denote such a flip plan by $\pi(T, T')$. If the valid linear-orderings of $\pi(T, T')$ are constrained flip paths, then this flip plan is constrained.

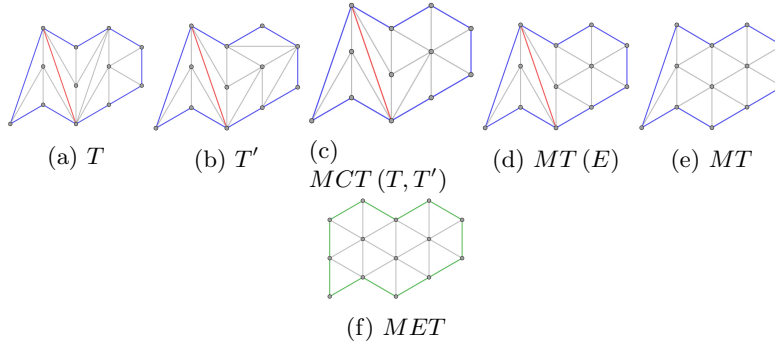


Figure 4: See Definition 4. (a) and (b) show two triangulations of a lattice point-set S with the blue bounding polygon containing the red edge. (c) shows the maximum common triangulation between the triangulations shown in (a) and (b). (d) shows the minimum triangulation containing the red edge (the singleton set E) and (e) shows the minimum triangulation. (f) shows the minimum equilateral triangulation, i.e., the minimum triangulation of a larger lattice point-set with the green bounding polygon.

We conclude this section by defining several unique triangulations of a lattice point-set with bounding polygon Ω .

Definition 4 (Unique Triangulations). *Let E be a set of edges. For some lattice point-set S with bounding polygon Ω , the following are unique triangulations of (S, Ω) (see Figure 4):*

- *the equilateral triangulation, if it exists, is the unique triangulation whose edges are of equal length. If this triangulation exists, then (S, Ω) is said to admit an equilateral triangulation.*
- *the Minimum Triangulation, denoted MT , is the unique triangulation whose total sum of edge lengths is minimum over all triangulations. Similarly, the minimum triangulation containing E , denoted by $MT(E)$, is the unique triangulation containing E whose total sum of edge lengths is minimum over all triangulations containing E .*
- *the Maximum Common Triangulation between any two triangulations T and T' of denoted by $MCT(T, T')$, is the minimum triangulation containing the edges common to both T and T' .*
- *the Minimum Equilateral Triangulation, denoted by MET , is the equilateral triangulation of a lattice point-set S' containing S , with bounding polygon Ω' containing Ω , that attains the minimum sum of edge lengths.*

If (S, Ω) as above admits an equilateral triangulation, it is clear that this triangulation is also the unique, minimum triangulation. The uniqueness of the other triangulations defined above are proved in Section 5.

2.2 Results and Organization

Refer to Figure 5.

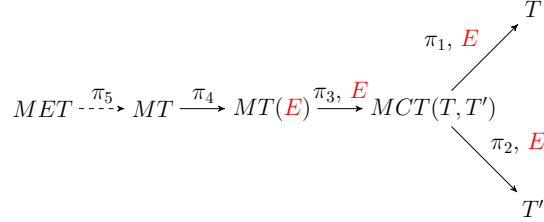


Figure 5: A sketch of the triangulations and minimum flip paths involved in our results. The set E is a set of constraints and the edges labelled π_1, π_2, π_3 , and π_4 denote minimum flip paths between pairs of triangulations defined in Definition 4. The dashed edge labelled π_5 denotes the computational cost, in terms of a number of flips, to describe the minimum triangulation from the minimum equilateral triangulation.

Theorem 1 (Unique, Minimum Flip Plan between Triangulations). *There is a unique, minimum flip plan constrained by a given set of edges E between any two triangulations. This flip plan consists of the flips in π_1 and π_2 . Furthermore, the flips in this flip plan and the partial order can be obtained in times*

$$O(|\pi_5| + |\pi_4| + |\pi_3| + |\pi_2| + |\pi_1|) \quad (1)$$

$$O(|\pi_1| \times |\pi_2|) \quad (2)$$

respectively.

Next, let $\Delta(E)$ denote the set of all triangulations containing a set of edges E . Also, observe that a triangulation can be uniquely specified by the set of edges that it contains.

Theorem 2 (Optimal Minimum Flip Plan Between Sets of Edges). *Consider triangulations U^* and V^* that contain sets of edges $E \cup G$ and $E \cup G'$ respectively. Also, consider the minimum flip plans, constrained by E , that generate the edges in G and G' from the minimum triangulation containing E respectively. Let π_1 and π_2 be these flip plans with their common flips removed. Then, the triangulations attain the minimum*

$$\min_{U \in \Delta(G), V \in \Delta(G')} |\pi(U, V)| \quad (3)$$

if and only if (i) the flips in the partial order π_1 (resp. π_2) are contained in the minimum flip plan for G (resp. G') and (ii) every edge generated by a flip in π_1 (resp. π_2) intersects some edge generated by a flip in the minimum flip plan for G' (resp. G).

We prove these theorems in Section 6. The necessary tools for these proofs are developed as follows.

1. Theorem 3 in Section 3, proved in our previous paper [20], shows that there is a unique, minimum flip plan that generates an edge from an equilateral triangulation.
2. Theorem 6 in Section 4 extends this result to a set of edges.
3. Theorem 7 in Section 5 gives the following:
 - an algorithm to compute the minimum triangulation from the minimum equilateral triangulation in $O(|\pi_5|)$ time
 - there is a unique, minimum flip plan, constrained by a set of edges E , that generates a set of edges G from the minimum triangulation containing E
 - the triangulation resulting from this constrained, minimum flip plan is a minimum triangulation containing $E \cup G$
4. Corollary 3 in Section 5 shows that the triangulations in Definition 4 and Figure 5 are unique.

We can treat the edges in Figure 5 as flip plans, rather than flip paths. Notice that the lattice point-set with bounding polygon Ω' of a minimum equilateral triangulation may strictly contain the original lattice point-set with bounding polygon Ω . Hence the edge labelled π_5 does not necessarily represent a flip plan between two triangulations, so it is dashed.

The main ideas in the proof of Theorem 1 are the following. Consider two triangulations T and T' , both containing a set of edges E . Theorem 7 allows us to compute the unique, minimum triangulation MT via the unique, minimum flip plan π_5 . Then, we can obtain the unique, minimum triangulation $MT(E)$ via the unique, minimum flip plan π_4 . By the same theorem, there are unique, minimum flip plans, constrained by E , between the minimum triangulation $MT(E)$ and the triangulations T and T' . The constrained, minimum flip plan π_3 is the maximum common subset of these flip plans, and it yields the maximum common triangulation $MCT(T, T')$. The key idea is that any minimum flip path between the triangulations T and T' can be reordered to pass through the maximum common triangulation $MCT(T, T')$. Finally, observe that the maximum common triangulation $MCT(T, T')$ must contain the edges in E , so such a minimum flip path is constrained by E .

Theorem 2 yields a simple algorithm for finding pairs of triangulations satisfying the minimization in Equation 3. Given any two triangulations U and V , containing a set of edges G and G' respectively, perform the flips in the flip plan $\pi(U, V)$ that preserve the sets of edges G and G' . This will yield two triangulations such that the minimum flip plan between them satisfies the conditions in Theorem 2.

Lastly, in Section 7 we give an application of our results in material science. We show how to model the propagation of cracks in crystalline materials caused by Stone-Wales defects, defined later. This physical phenomenon can be modeled by a minimum flip path that generates a set of edges from an equilateral triangulation. An edge in a triangulation represents a bond between atoms in the crystal and a flip corresponds to a Stone-Wales defect. However, this model results in a target triangulation with edges that are too long to represent atomic bonds. Theorem 8 shows that these long edges are unavoidable for an infinite family of edges. Thus, we propose to shorten these long edges by perturbing the points of the triangulations along the flip path and conjecture about suitable perturbation methods to accomplish this task.

Notably, all the above results follow from simple number-theoretic and geometric concepts, such as the connection between flip plans and Farey sequences [19] as elaborated in the next section.

3 Unique, Minimum Flip Plan for One Edge

In this section, we prove there is a unique, minimum flip plan that generates an edge at a point from an equilateral triangulation. A more expository proof of this result is given in [20].

Theorem 3 (Unique Minimum Flip Plan for an Edge). *On input edge e , Algorithm Flip Plan outputs the unique, minimum flip plan that generates an edge e from an equilateral triangulation.*

Proof idea: Theorem 4 shows that Algorithm *Flip Plan*, below, outputs a flip plan for an edge. This theorem follows directly from Theorem 5. Then, we use Corollary 2 to show that this is the unique, minimum flip plan for an edge.

A key observation that leads to Algorithm Flip Plan is the connection between an edge and the following elementary number-theoretic concept.

Definition 5 (Farey Sequence). *A Farey sequence [19] of order n , denoted by F_n , is a strictly-increasing sequence that lists all fully-reduced fractions (relatively prime pairs of nonnegative integers) in the range $[0, 1]$ with denominators of at most n .*

These sequences have several useful properties.

Property 1 (Mediant of Farey Neighbors). *For all $n > 1$, each fraction f_i in the Farey sequence F_n , except for the fractions $\frac{0}{1}$ and $\frac{1}{1}$, is the mediant of its Farey neighbors, which are the fractions f_{i-1} and f_{i+1} . In other words, if the fraction $\frac{x}{y}$ has Farey neighbors $\frac{a}{b}$ and $\frac{c}{d}$ in some Farey sequence, then $\frac{x}{y} = \frac{a+c}{b+d}$.*

Property 2 (Computing Farey Sequences). *Given a Farey sequence F_i , the Farey sequence F_{i+1} can be obtained by taking the mediant of each pair of consecutive terms in the Farey sequence F_i .*

Next we relate edges to fractions.

Definition 6 (Farey-Flip Map). *The Farey-Flip map ϕ_e is the map that takes an edge $e = (x, y)$ to the fraction $\frac{x}{y}$ if $x \leq y$, or to the fraction $\frac{y}{x}$ otherwise. The subscript is used to disambiguate between the two possible inverse maps.*

This map allows us to talk about a Farey sequence containing an edge e - i.e. a Farey sequence containing the fraction f that e is sent to via the Farey-Flip map ϕ_e . Let F_e denote the Farey sequence where e first appears. Likewise, we can talk about the Farey neighbor edges of the edge e , which are the edges obtained by applying the inverse Farey-Flip map ϕ_e^{-1} on the Farey neighbors of the fraction f in some Farey sequence.

Our first algorithm constructs the unique sequence of Farey fractions corresponding to an edge equivalence class.

Algorithm Farey Plan takes an edge $e = (x, y)$ as input and outputs its *Farey plan* C (one Farey plan for the equivalence class). The Farey plan C is initially empty. If the edge e is $(0, 1)$ or $(1, 0)$, then its Farey plan is empty. Otherwise, let the Farey-Flip map ϕ_e send the edge e to the fraction f , let the sequence X initially contain the Farey sequence F_1 , and let the fraction $d = \frac{1}{1}$. Repeat the following steps until the Farey plan C contains the fraction f .

1. Add the fraction d to the end of the Farey plan C . If C now contains f , output C .
2. Otherwise, if $f > d$, assign to d the mediant of d and the fraction directly after d in the sequence X ; otherwise, assign to d the mediant of d and the fraction directly before d in the sequence X .
3. Add d to the sequence X such that the sequence is in increasing order.

On an input edge e , this algorithm terminates in time linear in the order of the Farey sequence F_e and its output is unique by Properties 1 and 2. Next we define parallelograms from Farey neighbor edges.

Definition 7 (Farey Parallelogram for an Edge). *The Farey parallelogram for an edge e at a point v is the parallelogram containing e as its longer diagonal and whose boundary edges are copies of the Farey neighbor edges of e in the Farey sequence F_e , say e_1 and e_2 . This parallelogram is denoted by $P_{e,v} = \{e_1, e_2\}$.*

The nodes of the DAGs shown in Figure 3 are (flips performed on) Farey parallelograms. Note that the edge equivalence class induces an equivalence class of Farey parallelograms for the edge e , denoted by P_e . Likewise, we get the equivalence class of flips performed on the Farey parallelogram P_e .

Next, Lemma 1 describes the Farey plans of Farey neighbor edges and Lemma 2 describes the edges that compose Farey parallelograms.

Lemma 1 (Farey Plan of Longer Farey Neighbor Edge). *If an edge e has a Farey plan $C = \{f_1, \dots, f_n\}$, then applying the inverse Farey-Flip map ϕ_e^{-1} on the fraction f_{n-1} yields longer boundary edge e' in the Farey parallelogram for the edge e . Furthermore, the Farey plan for the edge e' is the sequence $C \setminus f_n$.*

Proof. This follows from Properties 1 and 2 □

Before stating the next lemma, define *adjacent copies of an edge e* to be an edge e at a point u and an edge e at a point v in a triangulation such that half of each of their Farey parallelograms share an edge. *Adjacent copies of the Farey parallelogram for e* are two such Farey parallelograms that share an edge. The edge equivalence class induces equivalence classes of adjacent copies of an edge e and adjacent copies Farey parallelograms for e .

Lemma 2 (Building on Longer Farey Neighbor Edges). *Let the edge e have Farey neighbor edges e_1 and e_2 in the Farey sequence F_e , let the Farey sequence F_{e_1} have higher order than the Farey sequence F_{e_2} , and let the shorter diagonal of the Farey parallelogram P_e be e_d . Then,*

- (i) *the Farey parallelogram $P_{e_1} = \{e_2, e_3\}$, for some edge e_3*
- (ii) *adjacent copies of the edge e_1 , whose adjacent Farey parallelograms share an edge e_3 , form the Farey parallelogram P_e and $e_d = e_3$*

Proof. For (i), simply observe that the edges e_1 and e_2 must be consecutive terms in the Farey sequence F_{e_1} , by Property 2. For (ii), the Farey parallelogram P_e contains one pair of the edges e_1 and e_2 both at the point $(0, 0)$ and another pair of the edges e_1 and e_2 both ending at some other point. By (i), the adjacent copies of the Farey parallelogram P_{e_1} described in the lemma clearly contain the boundary edges of the Farey parallelogram P_e , and we have $e_d = e_1 - e_2 = e_3$. □

Next we present our algorithm to compute a flip plan for an edge.

Algorithm *Flip Plan* takes an edge $e = (x, y)$ at a point v and its Farey plan $C = \{f_1, \dots, f_n\}$ as inputs and outputs a partially-ordered set of flips, denoted by $\pi_{e,v}$.

Base Cases: If the Farey plan C is empty, then the partial order $\pi_{e,v}$ is empty. If the fraction $f_n = \frac{1}{1}$, add a flip on the Farey parallelogram $P_{(1,1),v} = \{(0, 1), (1, 0)\}$ to the partial order $\pi_{e,v}$.

Recursive Step: Add a flip s on the Farey parallelogram $P_{e,v} = \{e_1, e_2\}$, obtained by applying the inverse Farey-Flip map ϕ_e^{-1} on the fractions f_{n-1} and $1 - f_{n-1}$, to the partial order $\pi_{e,v}$. Let the edge e_2 be the shorter boundary edge in the Farey parallelogram $P_{e,v}$. The children of the flip s are the root flips of the partial orders that result from recursing on the edge e_1 at the point v with Farey plan $C \setminus f_n$ and the edge e_1 at the point $v + e_2$ with Farey plan $C \setminus f_n$.

Clean-up Step: Finally, merge duplicate flips in the partial order $\pi_{e,v}$.

Our goal is now to prove the following theorem.

Theorem 4 (Flip Plan for an Edge). *On input edge e , Algorithm *Flip Plan* outputs a flip plan that generates e from an equilateral triangulation. Furthermore, this algorithm runs in time linear in the number of flips in this flip plan.*

The complexity statement in the theorem is clear from the steps in Algorithm Flip Plan. The fact that this algorithm outputs a flip plan follows directly from the following stronger theorem. We define *adjacent partially-ordered sets of flips* to be partial orders whose root Farey parallelograms are adjacent.

Theorem 5 (Flip Plan for Adjacent Copies of an Edge). *If π_e and π'_e are adjacent copies of the partially-ordered sets output by Algorithm Flip Plan on input edge e , then the set $\pi_e \cup \pi'_e$ is a flip plan that generates adjacent copies of the edge e from an equilateral triangulation.*

Next, we develop tools to prove this theorem. Corollary 1 is a consequence of Lemma 1 that describes the structure of the partial order output by Algorithm Flip Plan. Lemma 4 gives us a way to combine flip plans for certain edges into a flip plan for the set of these edges. This lemma is proved using Lemma 3.

Corollary 1 (Flip Plan for Longer Farey Neighbor Edge). *Let the partial order output by Algorithm Flip Plan on input edge e have a root flip with child flips s and w and let e' be the longer boundary edge of the Farey parallelogram for the edge e . The DAGs rooted at flips s and w are copies of the partial order output by Algorithm Flip Plan on input edge e' .*

Define the *bounding parallelogram* for an edge $e = (x, y)$ to be the parallelogram with boundary edges $\{(x, 0), (0, y)\}$, where these edges have the same defining coordinate pair as the edge e . Two edges whose bounding parallelograms do not have intersecting interiors are said to be *geometrically separated*.

Lemma 3 (Bounding Parallelogram Containment). *The Farey parallelograms in the partial order output by Algorithm Flip Plan on an input edge e are contained in the bounding parallelogram for the edge e .*

Proof. We proceed by induction on the size of the Farey plan for the edge e , say n . When $n = 1$, we have the edge $e = (1, 1)$, and the lemma holds. Assume the lemma holds for $n = k$ and we will show it holds for $n = k + 1$. Let π_e be the partial order output by Algorithm Flip Plan on input edge e . Clearly the root Farey parallelogram of π_e is contained in the bounding parallelogram for the edge e . Consider the longer boundary edge in the Farey parallelogram P_e , say e_k . By Lemma 1 and the inductive hypothesis, the Farey parallelograms in the partial order output by Algorithm Flip Plan on input edge e_k are contained in the bounding parallelogram for the edge e_k . Hence, by Corollary 1 and Lemma 2 the bounding parallelograms for the adjacent copies of the edge e_k , contained in the Farey parallelogram P_e , contain all the Farey parallelograms in the partial order π_e , except for the Farey parallelogram P_e . Lastly, by construction, the adjacent copies of the edge e_k have the same defining coordinate pair as the edge e , so their bounding parallelograms are contained in the bounding parallelogram for the edge e . Thus, the lemma is proved by induction. \square

Lemma 4 (Flip Plan for Geometrically Separated Edges). *Let $E = \{e_1, \dots, e_n\}$ be a set of edges such that every pair of edges is geometrically separated. Also,*

for each edge e_i in E , let the output of Algorithm Flip Plan on input edge e_i , denoted by π_{e_i} , be a flip plan that generates e_i from an equilateral triangulation. Then, $\pi_{e_1} \cup \dots \cup \pi_{e_n}$ is a flip plan that generates the set of edges E from an equilateral triangulation.

Proof. For each edge e_i in the set of edges E , the Farey parallelograms in the flip plan π_{e_i} are contained in the bounding parallelogram for e_i , by Lemma 3. Since every pair of edges in E is geometrically separated, no edge generated by a flip in the flip plan π_{e_i} can intersect with any edge generated by a flip in the flip plan π_{e_j} , for distinct edges e_i and e_j in E . Let $\pi_E = \pi_{e_1} \cup \dots \cup \pi_{e_n}$. Clearly any valid linear-ordering of π_E is a flip path for the set of edges E . Conversely, consider a flip path for the set of edges E that contains the flips in π_E . This flip path consists of subsequences of flips that form valid linear-orderings of the flip plans $\pi_{e_1}, \dots, \pi_{e_n}$, by assumption. Thus, this flip path is a valid linear-ordering of π_E and the lemma is proved. \square

Now we can prove Theorem 5.

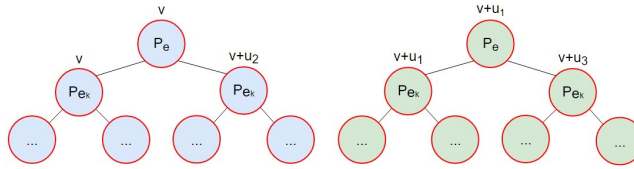


Figure 6: The partial orders and flip plan described in Theorem 5 are shown in blue, green, and red respectively. The value of u_1 is such the partial orders are adjacent.

Proof of Theorem 5. We proceed by induction on the size of the Farey plan for the edge e , say n . When $n = 1$, the theorem is easily verified for the edge $e = (1, 1)$. Assume that the theorem holds for $n = k$ and we will prove it holds for $n = k + 1$. Refer to Figure 6, which shows adjacent copies of the partial order output by Algorithm Flip Plan on input edge e . Denote the partial order in blue by π_e , the one in green by π'_e , and the one in red by $\pi_e \cup \pi'_e$.

Corollary 1 tells us that e_k is the longer boundary edge in the Farey parallelogram P_e . By Lemma 1 and the inductive hypothesis, the partial order π_e with its maximal flip removed is a flip plan for adjacent copies of the edge e_k . Hence, by Lemma 2, this flip plan generates the boundary edges of the Farey parallelogram P_e and its shorter diagonal. Furthermore, since the adjacent copies of the Farey parallelogram for e_k must not contain lattice points in their interiors, the Farey parallelogram P_e does not contain a lattice point in its interior. Hence, the maximal flip in π_e can be performed, so π_e is a flip plan for the edge e . Similarly, π'_e is a flip plan for the edge e . Now we must show that $\pi_e \cup \pi'_e$ is a flip plan for adjacent copies of the edge e .

For one direction, assume a flip path for adjacent copies of the edge e that contains the flips in the partial order $\pi_e \cup \pi'_e$ is not one of its valid linear-



Figure 7: The different possibilities for the edge e in the proof of Theorem 5. (a) shows two pairs of adjacent copies of the Farey parallelogram P_{e_k} : one pair sharing a purple edge the other sharing a green edge. These result in two different Farey parallelograms for the edge e , and hence two different possibilities for the edge e .

orderings. Then, some flip s in the partial order $\pi_e \cup \pi'_e$ is performed before a flip in the DAG rooted at s . Let s be the lowest level flip satisfying this condition. At least one child flip of s has not been performed, so by Corollary 1 and Lemma 2 the Farey parallelogram that the flip s is performed on has not been generated. Hence, the flip s cannot be performed and we get a contradiction. Thus, this flip path is a valid linear-ordering of the partial order $\pi_e \cup \pi'_e$.

For the other direction, we must show that a valid linear-ordering of the partial order $\pi_e \cup \pi'_e$ is a flip path for adjacent copies of the edge e . Consider the Farey parallelograms for the adjacent copies of the edge e_k contained in the Farey parallelogram P_e . There are two cases for the edge e resulting from the choice of the edge shared between these adjacent Farey parallelograms (see Figure 7). This leads to four cases for the possible configurations of the adjacent copies of the edge e , as shown in Figure 8. The copies of the edge e_k are labelled in these cases. By the inductive hypothesis, each DAG rooted at a Farey parallelogram P_{e_k} in $\pi_e \cup \pi'_e$ is a flip plan for a copy of the edge e_k . For the edge labelled i , let π_i denote the flip plan for this edge. In cases (a) and (d), let $\pi^* = \pi_1 \cup \pi_2 \cup \pi_3 \cup \pi_4$, and in cases (b) and (c) let $\pi^* = \pi_1 \cup \pi_2 \cup \pi_3$. In other words, π^* is the partial order $\pi_e \cup \pi'_e$ with its two maximal flips removed.

In each case, it suffices to show that the partial order π^* is a flip plan that generates each pair of the copies of the edge e_k . We justify this claim at the end. For one direction, assume some flip path for each pair of the copies of the edge e_k that contains the flips in π^* is not one of its valid linear-orderings. This flip path must contain a flip path for one of the copies of the edge e_k , say the one labelled i , that is not a valid linear-ordering of the flip plan π_i , which is a contradiction. For the other direction, it suffices to show that $\pi_i \cup \pi_j$ is a flip plan for the edges labeled i and j , for each pair of these edges. In all cases, $\pi_i \cup \pi_j$ is a flip plan for all adjacent pairs of edges, by Lemma 1 and the inductive hypothesis. Note that in cases (a) and (d) this includes the flip plans whose root Farey parallelograms originate at the points $v + u_1$ and $v + u_2$ (Figure 6), while in cases (b) and (c) these flip plans are the same. In cases (b) and (c), $\pi_1 \cup \pi_3$

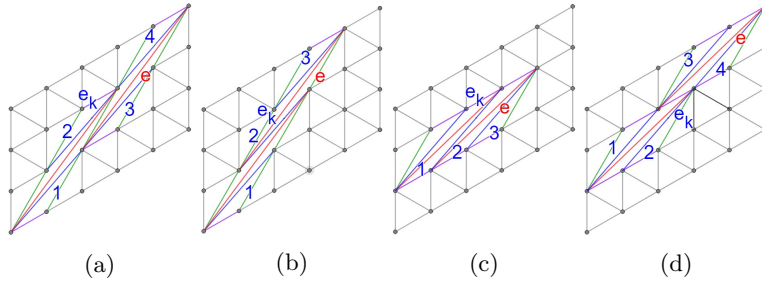


Figure 8: The cases of the adjacent copies of the edge e in the proof of Theorem 5.

is a flip plan for the pair of edges labelled 1 and 3 by transitivity. Finally, for cases (a) and (d), the pairs of edges labelled 1 and 3, 1 and 4, and 2 and 4 are geometrically separated, so $\pi_1 \cup \pi_3$, $\pi_1 \cup \pi_4$, and $\pi_2 \cup \pi_4$ are flip plans for these respective pairs of edges by Lemma 4.

Now we justify the claim above. Suppose π^* is a flip plan that generates each pair of the copies of the edge e_k , but some valid linear-ordering of the partial order $\pi_e \cup \pi'_e$ is not a flip path for adjacent copies of the edge e . This ordering consists of a flip path p for the copies of the edge e_k and two flips on the adjacent copies of the Farey parallelogram P_e , such that each of these two flips is performed somewhere along p . Since p is a valid linear-ordering of π^* , the first flip that cannot be performed must be on one of the copies of the Farey parallelogram P_e . By Lemma 2, the Farey parallelogram P_e is contained in the triangulation immediately prior to this flip. This means that the edge e resulting from this flip must intersect some edge g in this triangulation, other than the shorter diagonal of the Farey parallelogram P_e . Also, the edge g intersects a boundary edge of the Farey parallelogram P_e . However, the interiors of the adjacent copies of the Farey parallelogram P_e are disjoint, so the edge g must be generated by some flip in the flip path p , which is a contradiction. Hence, this flip can be performed. By similar reasoning, the remaining flips in this ordering, including the flip on the other Farey parallelogram P_e , can be performed after this flip. Thus, the ordering is a flip path for adjacent copies of the edge e and the theorem is proved by induction. \square

Lastly, we prove Lemma 5, which yields Corollary 2. With this last tool, we can prove Theorem 3.

Lemma 5 (Uniqueness of Parallelograms). *The Farey parallelogram for an edge e is the unique parallelogram, with lattice points as vertices and the edge e as its longer diagonal, whose interior is free of lattice points.*

Proof. One direction follows from Theorem 4. For the other direction, note that by definition the Farey neighbor edges of the edge e in the Farey sequence F_e are the unique pair of edges that are shorter than e and whose slopes are closest to the slope of e from either side. Consider some parallelogram P_e , with

lattice points as vertices and e as its longer diagonal, that is not the Farey parallelogram for the edge e . If P_e contains the Farey parallelogram, then we are done. Otherwise, one of the boundary edges of P_e , say $g = (x, y)$, is shorter than the edge e and has a slope that is closest to the slope of e from one side. Since the edge g is not a Farey neighbor edge of e , then x and y must not be relatively prime integers so that one of the vertices of the parallelogram P_e is not a lattice point. This contradicts our assumption. Thus, the interior of the parallelogram P_e contains a lattice point. \square

Corollary 2 (Uniqueness of Quadrilaterals). *The Farey parallelogram for an edge e is the unique quadrilateral, with lattice points as vertices and the edge e as its longer diagonal, whose interior is free of lattice points.*

Proof. By Lemma 5, the Farey parallelogram for the edge e does not contain a lattice point in its interior. By the same lemma, it is clear that any other quadrilateral, with lattice points as vertices and the edge e as its longer diagonal, contains a lattice point in at least one half of its interior. \square

Proof of Theorem 3. A flip plan π_e for an edge e can be obtained via Theorem 4. Corollary 2 tells us that every flip plan for the edge e consists of Farey parallelograms. Finally, by Corollary 1 and Lemma 2, each flip in π_e is necessary for its parent flip, and the root flip is necessary to generate e . Thus, any minimum flip plan for the edge e must contain the flips in the flip plan π_e . \square

4 Unique, Minimum Flip Plan for Multiple Edges

In this section, we prove there is a unique, minimum flip plan that generates a set of non-intersecting edges at a set of points from an equilateral triangulation. We will use the fact that triangulations are maximally planar graphs, meaning that if two edges do not intersect at a point other than their endpoints, then they are both contained in some triangulation. The following algorithm constructs the desired flip plan.

Algorithm Multi Flip Plan takes a set of edges E at a set of points V as input and outputs the partially-ordered set of flips $\pi_E = \pi_{e_1} \cup \dots \cup \pi_{e_{|E|}}$, where π_{e_i} is the minimum flip plan for the edge e_i in E . These minimum flip plans are obtained by running Algorithms Farey Plan and Flip Plan on each edge in E . Flip plans with flips in common are merged in the obvious way - e.g. Figure 9 shows the minimum flip plans for the edges (1,3) and (1,2) both at the point (0,0), which have been merged at their common flips.

Theorem 6 (Unique, Minimum Flip Plan for Multiple Edges). *On an input set of edges E , Algorithm Multi Flip Plan outputs the unique, minimum flip plan that generates the edges in E from an equilateral triangulation. Furthermore, this algorithm runs in time linear in the number of flips in this flip plan.*

Proof idea: Let π_E denote the partially-ordered set of flips output by Algorithm Multi Flip Plan on an input set of edges E . Lemma 7 is used to show that

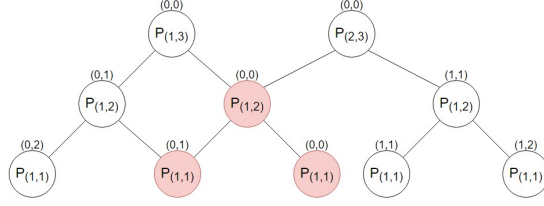


Figure 9: The intersection of the minimum flip plans for edges $(1, 3)$ and $(2, 3)$, both at the point $(0, 0)$ and defined by the same defining coordinate pair. If these edges were defined using different defining coordinate pairs, then the only Farey parallelograms that could be in the intersection are copies of $P_{(1,1)}$. See Section 4.

π_E is a flip plan for E . This lemma is proved using Lemma 6. Minimality and uniqueness of π_E will follow from Theorem 3. Lastly, the complexity statement follows from repeatedly applying Theorem 4.

Lemma 6 (Farey Parallelogram Containment). *Every Farey parallelogram in the minimum flip plan that generates an edge e from an equilateral triangulation contains the edge e in its interior.*

Proof. We proceed by induction on the size of the Farey plan for the edge e , n . When $n = 1$, the edge $e = (1, 1)$, so the lemma holds. Assume the lemma holds when $n = k$ and we will show it holds for $n = k + 1$. Clearly the Farey parallelogram P_e contains the edge e in its interior. Let e_k be the longer boundary edge in the Farey parallelogram P_e . By Lemma 1 and the inductive hypothesis, all Farey parallelograms in the flip plan for the edge e_k contain the edge e_k in their interiors. Consider the adjacent copies of the edge e_k contained in the Farey parallelogram P_e , according to Lemma 2. By Corollary 1, if there is a Farey parallelogram in the flip plan for either of these edges that does not contain the edge e in its interior, then the Farey parallelogram P_e contains a lattice point in its interior. This contradicts Corollary 2. Thus, the lemma is proved by induction. \square

Lemma 7 (Flip Path for Edges in a Sequence). *Given a sequence of non-intersecting edges $E = \{e_1, \dots, e_n\}$ and, for each edge e_i in E , the unique, minimum flip plan π_{e_i} that generates e_i from an equilateral triangulation, any valid linear-ordering of the partially-ordered set $\pi_{e_1} || \dots || \pi_{e_n}$ is a flip path that generates the edges in E from an equilateral triangulation in sequential order.*

Proof. We proceed by induction on the number of edges in the sequence, say n . When $n = 1$, the lemma holds by Theorem 3. Assume that the lemma holds when $n = k$, and we will show that it holds for $n = k + 1$. Let e_1, \dots, e_k, e_{k+1} be a sequence of $k + 1$ edges. By the inductive hypothesis, any valid linear-ordering of the partial order $\pi_k = \pi_{e_1} || \dots || \pi_{e_k}$ is a flip path that generates the first k edges from an equilateral triangulation in sequential order. Let the edge

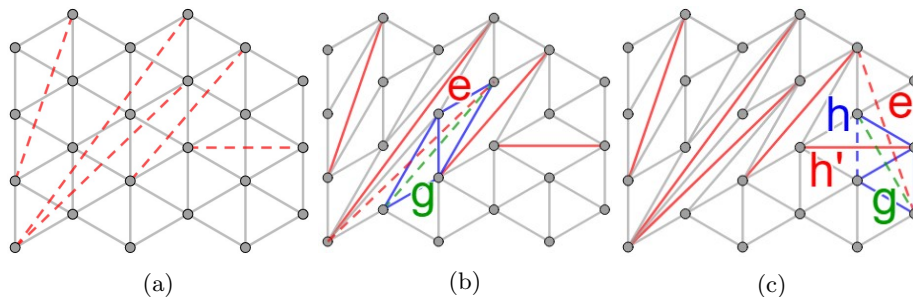


Figure 10: See the proof of Lemma 7. (a) shows the set of edges E to be generated in red. (b) shows the inductive step where e is the next edge in E to be generated, g is the edge resulting from the flip s to be performed, and the blue edges make up the Farey parallelogram g and its shorter diagonal. (c) shows the contradiction arising in the proof. In the image, the edge h' is the same as the edge e' , but this is not always the case.

$e = e_{k+1}$ and let π_e be the minimum flip plan for e . It suffices to show that the flips in any valid linear-ordering of the minimum flip plan π_e can be performed after the flips in any valid linear-ordering of the partial order π_k .

If the minimum flip plan π_e is a subset of the partial order π_k , then we are done. Otherwise, consider a flip s in the minimum flip plan π_e such that all flips in the DAG rooted at s have been performed, except for s . It suffices to show that the flip s can be performed, because s cannot prevent a later flip in a valid linear-ordering of the flip plan π_e from being performed, by definition. Let g be the edge generated by the flip s . Equivalently, we will show that the boundary edges of the Farey parallelogram for g and its shorter diagonal are contained in the triangulation T immediately prior to the flip s . Then, by Corollary 2, the flip s can be performed.

Assume to the contrary that one of the above-mentioned edges contained in the Farey parallelogram for g , say h , is not contained in the triangulation T . If h is a boundary edge of the Farey parallelogram for g , then h was flipped to yield a longer edge h' (see Figure 10). Hence, h' is either one of the first k edges in the sequence or, by Corollary 1, the longer boundary edge of some Farey parallelogram contained in the minimum flip plan for one of the first k edges in the sequence, say e' . Each flip in the minimum flip plan $\pi_{e'}$ is necessary for its parent flip by Corollary 2 and Lemma 2. Hence, the flip generating the edge h' is necessary to generate the edge e' . Now, by Lemma 6, the Farey parallelogram for the edge h' contains the edge e' . In order to flip the edge h' to yield the edge h , we must first flip the edge e' to yield a shorter edge. This means that the edges e and e' cannot simultaneously exist in a triangulation. Thus, the edges e and e' must intersect, which contradicts our assumption.

Lastly, if the edge h is the shorter diagonal of the Farey parallelogram for the edge g , then by Lemma 2 some boundary edge of the Farey parallelogram for g is not contained in the triangulation T and we get a similar contradiction.

Hence, the boundary edges of the Farey parallelogram for g and its shorter diagonal are contained in T . Thus, the flip s can be performed and the lemma is proved by induction. \square

Proof of Theorem 6. First, we show that any valid linear-ordering of the partial order $\pi_E = \pi_{e_1} \cup \dots \cup \pi_{|E|}$ is a flip path for the edges in E . Such an ordering is an interleaving of minimum flip paths for the edges in E . Hence, we can partition the ordering into subsequences of these minimum flip paths. For each subsequence, consider the highest level flips in the corresponding flip plan that it contains. The DAGs rooted at these flips are minimum flip plans for non-intersecting edges. Iterating over the subsequences yields a sequence of these minimum flip plans for non-intersecting edges. Applying Lemma 7 to this sequence proves this direction.

Next, we show that any flip path for the edges in E that contains the flips in the partial order π_E is one of its valid linear-orderings. Assume this is not the case. Then, some flip s in the minimum flip plan for an edge e in E is performed before a flip in the DAG rooted at s . Consider the lowest level flip satisfying this condition. By Corollary 1 and Lemma 2, the Farey parallelogram that the flip s is performed on does not exist in the triangulation immediately prior to s . Hence, this flip cannot be performed, which is a contradiction. Thus, π_E is a flip plan for the edges in E .

Lastly, the flip plan π_E consists of unique, minimum flip plans by Theorem 3, and the roots of these minimum flip plans are maximal elements. Thus, π_E must be the unique, minimum flip plan for the edges in E and the complexity statement follows from repeatedly applying Theorem 4. \square

5 Unique, Minimum Flip Plans Starting from Any Minimum Triangulations

In this section, we show there is a unique, minimum flip plan, constrained by a set of edges E , that generates a set of edges G from a minimum triangulation containing E . We begin with the case where (S, Ω) admits an equilateral triangulation, for some lattice point-set S with bounding polygon Ω .

Lemma 8 (Minimum Flip Plans Yield Minimum Triangulations). *If (S, Ω) admits an equilateral triangulation, then the minimum flip plan that generates a set of edges E from this equilateral triangulation yields the unique, minimum triangulation containing E .*

Proof. Note that every triangulation T containing the set of edges E can be specified by the set of all edges $H = E \cup G$ contained in T . By Theorem 6, there is a unique, minimum flip plan for the edges in H , denoted by $\pi_H = \pi_E \cup \pi_G$. All of the flips in this flip plan are length-increasing by construction. Thus, the triangulation resulting from the unique, minimum flip plan π_E is the unique, minimum triangulation containing E . \square

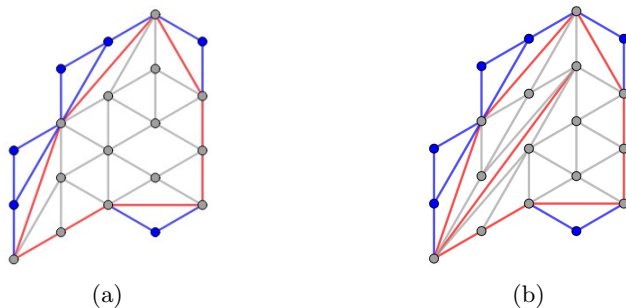


Figure 11: See the proof of Theorem 7. The boundary edges of Ω are in red and the vertices and edges to be removed are in blue. (a) shows the minimum triangulation of (S', Ω') containing the boundary edges of Ω . (b) shows the minimum triangulation of (S', Ω') containing the boundary edges of Ω and an additional red edge, i.e., the singleton set of constraints E .

Before we can extend this result to the case when (S, Ω) does not admit an equilateral triangulation, we must be able to describe its minimum triangulation. We first establish the uniqueness of the minimum equilateral triangulation.

Lemma 9 (Uniqueness of Minimum Equilateral Triangulations). *The minimum equilateral triangulation of a lattice point-set S with bounding polygon Ω is unique.*

Proof. For any lattice point-set S with bounding polygon Ω , consider the minimum flip plan that generates the boundary edges of Ω from an equilateral triangulation. The flips in this flip plan determine the unique lattice point-set S' with bounding polygon Ω' , in Definition 4, whose equilateral triangulation attains the minimum sum of edge lengths. Since the equilateral triangulation of (S', Ω') is unique, the lemma is proved. \square

Now we extend Theorem 6 and Lemma 8 to lattice point-sets S with bounding polygons Ω that do not admit equilateral triangulations.

Theorem 7 (Unique, Minimum Flip Plan from Any Minimum Triangulation). *Given a lattice point-set S with bounding polygon Ω , a set of edges $H = E \cup G$, and the minimum flip plan $\pi_{\Omega \cup H}$ that generates the boundary edges of Ω and the edges in H from an equilateral triangulation, the following statements hold:*

- (i) *the minimum triangulation is unique and can be obtained from the minimum equilateral triangulation in $O(|\pi_{\Omega}(MET)|)$ time by performing the following steps:*
 - (a) *use the minimum flip plan $\pi_{\Omega \cup H}$ to generate the boundary edges of Ω from the minimum equilateral triangulation*
 - (b) *remove the vertices and edges from the resulting triangulation that are not contained in (S, Ω)*

(ii) the remaining flips in the minimum flip plan $\pi_{\Omega \cup H}$ make up the unique, minimum flip plan $\pi_H(MT)$ that generates the edges in H from the minimum triangulation. Furthermore, this flip plan yields the unique, minimum triangulation containing H .

(iii) The set of edges E can be generated from the minimum triangulation first and the remaining flips in the minimum flip plan $\pi_H(MT)$ make up the unique, minimum flip plan, constrained by E , that generates the edges in G from the minimum triangulation containing E . Furthermore, this flip plan yields the minimum triangulation containing $E \cup G$.

Proof. Refer to Figure 11. For (i), let S' be the lattice point-set with bounding polygon Ω' for the minimum equilateral triangulation. By Lemma 9, (S', Ω') is unique. The triangulation resulting from Step (a) is the unique, minimum triangulation of (S', Ω') containing the boundary edges of Ω , by Lemma 8. The triangulation resulting from Step (b) is clearly a minimum triangulation of (S, Ω) . Any other minimum triangulation of (S, Ω) yields another minimum triangulation of (S', Ω') containing the boundary edges of Ω , by reversing Step (b). Thus, by Lemma 9 the triangulation resulting from Steps (a) and (b) is the unique, minimum triangulation of (S, Ω) . Lastly, by Theorem 6, the minimum flip plan for the boundary edges of Ω can be computed in $O(|\pi_{\Omega}(MET)|)$ time.

For (ii), observe that the flips remaining in the minimum flip plan $\pi_{\Omega \cup H}$ after generating the boundary edges of Ω from the minimum equilateral triangulation consist of Farey parallelograms that are contained in (S, Ω) . Hence, these flips make up the unique, minimum flip plan $\pi_H(MT)$ that generates the set of edges H from the minimum triangulation.

Next, modify Step (a) in the algorithm from (i) to perform all flips in the minimum flip plan $\pi_{\Omega \cup H}$. By Lemmas 8 and 9, the triangulation resulting from this modified Step (a) is the unique, minimum triangulation of (S', Ω') containing the boundary edges of Ω and H . Hence, performing Step (b) yields a minimum triangulation of (S, Ω) containing H . Clearly the minimum flip plan $\pi_H(MT)$ yields this minimum triangulation. Similarly to the proof of (i), any other minimum triangulation of (S, Ω) containing H yields another minimum triangulation of (S', Ω') containing the boundary edges of Ω and H , by reversing Step (b). Thus, the minimum triangulation of (S, Ω) containing H is unique.

For (iii), by Theorem 6, the partial order of the minimum flip plan $\pi_{\Omega \cup H}$ allows each edge to be generated independently of the other edges. The minimum flip plan $\pi_H(MT)$ is a subset of the minimum flip plan $\pi_{\Omega \cup H}$ that preserves this property. Hence, the edges in E can be generated from the minimum triangulation first. By (ii), the resulting triangulation is the minimum triangulation containing E . Thus, the flips remaining in the minimum flip plan $\pi_H(MT)$ after generating the edges in E make up the unique, minimum flip plan $\pi_G(MT(E))$, constrained by E , that generates the edges in G from the minimum triangulation containing E . Finally, generating the edges in E first does not change the triangulation resulting from the minimum flip plan $\pi_H(MT)$, so the minimum flip plan $\pi_G(MT(E))$ yields the minimum triangulation containing $E \cup G$. \square

We end this section with a corollary of Theorem 7.

Corollary 3 (Unique Triangulations). *The triangulations given in Definition 4 are unique.*

Proof. These triangulations are all minimum triangulations containing different sets of edges, so they are unique by Theorem 7. \square

6 Unique, Minimum Flip Plan Between Two Triangulations

In this section, we prove Theorems 1 and 2. We also give an algorithm to compute a minimum flip path between two triangulations and analyze its complexity. Let T and T' be triangulations of (S, Ω) that contain the sets of edges $E \cup G$ and $E \cup G'$ respectively, for some lattice point-set S with bounding polygon Ω . Refer to Figure 5.

Algorithm Tri Flip Plan takes the sets of edges G and G' as input and outputs a partially-ordered set of flips $\pi(T, T')$. The algorithm performs the following steps:

1. Apply Theorem 7 to obtain the unique, minimum flip plans, constrained by E , that generate the edges in G and G' from the minimum triangulation containing a set of edges E respectively. The former minimum flip plan contains the flips in π_3 and π_1 and the latter contains the flips π_3 and π_2 from Figure 5.
2. Remove the flips π_3 shared between these minimum flip plans to get the sets π_1 and π_2 respectively.
3. Recall that an edge in the DAG of a flip plan is always pointing towards a parent node. Reverse the direction of each edge in the DAG of π_1 , so that the highest level is now the lowest level and flips generate shorter diagonals of Farey parallelograms. Denote this partial order by π_1^{-1} .
4. Let $\pi_{2,g'}$ denote the portion of the constrained, minimum flip plan for an edge g' in G' contained in the set π_2 . We will insert the set $\pi_{2,g'}$ into the set π_1^{-1} as follows. For each edge g' in G' such that the set $\pi_{2,g'}$ is not empty, consider each leaf Farey parallelogram P_h , for some edge h , in the set $\pi_{2,g'}$. Find the Farey parallelograms in the set π_1^{-1} whose longer diagonals intersect h . Set these Farey parallelograms to be children of the Farey parallelogram P_h . If no child flips are assigned this way, then the Farey parallelogram P_h remains a leaf Farey parallelogram in the set π_1^{-1} .

The partial order resulting from these DAG insertions is the output.

Figure 12 shows the unique, minimum flip plan output by Algorithm Tri Flip Plan between a triangulation containing the edge $(2, 3)$ at the point $(0, 0)$

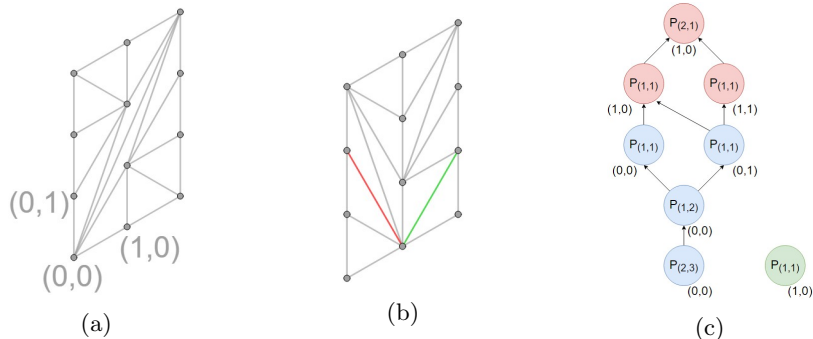


Figure 12: (c) is the unique, minimum flip plan between the triangulations in (a) and (b). The red and green edges in (b) correspond to the red and green Farey parallelograms $P_{(1,1),(1,0)}$ in (c). For clarity, not all of the arrows between the red leaf flips and their blue child flips are shown, but these are clear from the triangulations.

and a triangulation containing the edge $(2, 1)$ at the point $(1, 0)$, the edge $(1, 1)$ at the point $(1, 0)$, and the edge $(1, 2)$ at the point $(1, 1)$. The set π_1^{-1} from Step 3 is shown in blue. The sets $\pi_{2,(1,1)}$ and $\pi_{2,(2,1)}$ are shown in green and red respectively. The single flip in the former set can be performed at any time, but the flips in the latter set must be performed after the maximal flips in the set π_1^{-1} . Note that the edge $(1, 2)$ at the point $(1, 1)$ is contained in both triangulations, so the flips in its the minimum flip plan are not contained in the minimum flip plan between these triangulations.

We now prove Theorem 1.

Proof of Theorem 1. Refer to Figure 5. We demonstrate the following: (i) the partial order $\pi(T, T')$ output by Algorithm Tri Flip Plan on input sets of edges G and G' does not contain any flip in the minimum flip plan for the constraint edges E , (ii) any minimum flip path between the triangulations T and T' contains the flips in $\pi(T, T')$, and (iii) $\pi(T, T')$ is a flip plan between T and T' . Statement (i) implies that the flip paths in (ii) are constrained by E . Combining (i), (ii), and (iii) shows that the partial order $\pi(T, T')$ is the unique, minimum flip plan, constrained by E , between the triangulations T and T' . Finally, we will prove Complexity Statements 1 and 2.

For (i), Step 1 of the algorithm yields the unique, minimum flip plans $\pi_G(MT(E))$ and $\pi_{G'}(MT(E))$ constrained by E , by Theorem 7. The partial order of common flips between these minimum flip plans, π_3 , is itself a constrained, minimum flip plan for a set of edges. By definition, the triangulation resulting from π_3 is the maximum common triangulation $MCT(T, T')$. Hence, the sets of flips π_1 and π_2 in Step 2 of the algorithm are the unique, minimum flip plans, constrained by E , between the triangulation $MCT(T, T')$ and the triangulations T and T' respectively. Furthermore, since π_1 and π_2 are subsets of the constrained, minimum flip plans $\pi_G(MT(E))$ and $\pi_{G'}(MT(E))$,

they are also constrained by E .

For (ii), consider the set π_1^{-1} resulting from Step 3 of the algorithm, which reverses the flips in the minimum flip plan π_1 . Any minimum flip path between the triangulations T and T' can be partitioned into subsequences of flips that either generate or reverse the generation of edges. Since the triangulation $MCT(T, T')$ is unique, by Corollary 3, it suffices to show that we can reorder any such minimum flip path so that all of the degenerating subsequences of flips are performed prior to the generating subsequences of flips. If this is true, then clearly the degenerating and generating sequences of flips form valid linear-orderings of the minimum flip plans π_1^{-1} and π_2 respectively.

Assume to the contrary that some degenerating subsequence of flips cannot be performed prior to a generating subsequence of flips. Then, the minimum flip path contains a length-increasing flip s that must be performed prior to a length-decreasing flip w . In particular, we can choose the flips s and w such that there is no other pair of flips satisfying this condition between them in the minimum flip path. Hence, we can reorder the minimum flip path such that the flip s is performed immediately prior to the flip w .

Now, let U_1 be the triangulation immediately prior to the flip s in the minimum flip path. By Theorem 7, there is a unique, minimum flip plan, constrained by E , that generates the edges contained in the triangulation U_1 from the minimum triangulation containing E . Denote this minimum flip plan by $\pi(U_1)$. By Lemma 6, length-decreasing flips can only be performed on maximal elements of minimum flip plans for edges. Hence, the flip w must not be a maximal element in the minimum flip plan $\pi(U_1)$. The length-increasing flip s generates an edge from U_1 , so the minimum flip plan $\pi(U_1)$ is a subset of the minimum flip plan $\pi(U_2)$, where U_2 is the triangulation resulting from the flip s . The length-decreasing flip w is a maximal element in $\pi(U_2)$, so w must reverse the length-increasing flip s . Clearly, we can remove the flips s and w from the minimum flip path and obtain a flip path between the triangulations T and T' containing 2 fewer flips. This is a contradiction, so the flip w can be performed prior to the flip s .

For (iii), in one direction consider some valid linear-ordering of the partial order $\pi(T, T')$. We show that this ordering is a flip path between the triangulations T and T' by demonstrating that the first n flips in this ordering can be performed. We proceed by induction on n . When $n = 1$, the first flip is contained in either the set π_1^{-1} or the set $\pi_{2, g'}$, for some edge g' in G' . In the former case, the flip can be performed in the triangulation T , since π_1^{-1} is the minimum flip plan between T and the triangulation $MCT(T, T')$. In the latter case, the edge h' generated by this flip does not intersect any longer diagonal of a Farey parallelogram in the set π_1^{-1} , by construction. Hence, there is a minimum flip plan that generates the edges in $G \cup h'$ from the minimum triangulation containing E , by Theorem 7. Furthermore, the edge h' can be generated last. Thus, the base case holds.

Assume the claim holds for $n = k$ and we will show that it holds for $n = k + 1$. By the inductive hypothesis, we can perform the first k flips of this ordering, which yield a triangulation represented by a set of edges H . The $(k + 1)^{\text{th}}$ flip is

the first flip in a valid linear-ordering of the partial order output by Algorithm Tri Flip Plan on input edges H and G' , so the argument for the base case applies. Thus, the claim is proved by induction.

For the other direction, assume that some minimum flip path between the triangulations T and T' that contains the flips in the partial order $\pi(T, T')$ is not a valid linear-ordering of this partial order. Then either (a) some subsequence of this minimum flip path is not a valid linear-ordering of the set π_1^{-1} or the set $\pi_{2,g'}$, for some edge g' in G' , or (b) some leaf flip s in the set $\pi_{2,g'}$ is performed before one of its child flips in the set π_1^{-1} . In case (a), some flip in this flip path cannot be performed, by Theorem 7, which is a contradiction. In case (b), the edge generated by the leaf flip s intersects with the longer diagonal of some Farey parallelogram in the set π_1^{-1} . If this longer diagonal exists in the triangulation when the leaf flip s is meant to be performed, then s cannot be performed. Otherwise, after the leaf flip s is performed, the flip in π_1^{-1} that yields the intersecting diagonal cannot be performed. In either situation we get a contradiction.

Finally, for Complexity Statement 1, in order to obtain the minimum flip plans π_1^{-1} and π_2 , we must first compute the minimum triangulation. This can be done in $O(|\pi_5|)$ time, by Theorem 7. The minimum flip plan that generates the edges in E from this triangulation is a subset of the minimum flip plan that generates the edges in E from an equilateral triangulation. By Theorem 6, this minimum flip plan can be computed in $O(|\pi_4|)$ time. Similarly, we can compute the minimum flip plans $\pi_G(MT(E))$ and $\pi_{G'}(MT(E))$ in $O(|\pi_3| + |\pi_2| + |\pi_1|)$ time. Lastly, the flips in the set π_1 can be reversed in $O(|\pi_1|)$ time. Putting it all together proves Complexity Statement 1. For Complexity Statement 2, Step 4 of the algorithm clearly uses at most this much time. \square

Complexity Statement 2 is the result of the work done in Step 4 of Algorithm Tri Flip Plan to compute the partial order of the flip plan between two triangulations T and T' . Observe that a valid linear-ordering of the set $\pi_1^{-1}||\pi_2$ is a minimum flip path between the triangulations T and T' . Hence, Steps 1 - 3 of this algorithm are sufficient to compute a minimum flip path between two triangulations and we get the following algorithm.

Algorithm Tri Flip Path has the same input parameters as Algorithm Tri Flip Plan, performs Steps 1 - 3 of Algorithm Tri Flip Plan, and then outputs a valid linear-ordering of the set $\pi_1^{-1}||\pi_2$.

As a direct consequence of Theorem 1, Algorithm Tri Flip Path runs in the time given by Complexity Statement 1. The following lemma from Caputo et al. [2] can be used to analyze the time complexity of Algorithm Tri Flip Path.

Lemma 10 (Minimum Flip Path Bound). *The number of flips in any minimum flip path between two triangulations of an $m \times n$ lattice point-set is $O(mn(m+n))$.*

Proposition 1 (Worst-Case Complexity). *Consider two triangulations whose non-unit length edges are contained in an $m \times m$ subregion of an $n \times n$ lattice*

point-set. Algorithm Tri Flip Path computes a minimum flip path between these two triangulations in $O(m^3)$ time.

Proof. By Lemma 3, the flips in the minimum flip plan between these two triangulations are contained in the $m \times m$ subregion. Observe that each term in Complexity Statement 1 is the number of flips in a minimum flip plan between two triangulations of this subregion. Applying Lemma 10 to each term yields the desired complexity. \square

In the worst case, Algorithm Tri Flip Path runs in $O(n^3)$ time, but for sufficiently small values of m the complexity is much better. The following proposition shows that in many cases, Algorithm Tri Flip Path runs in time linear in the size of its output. Refer to Figure 5.

Proposition 2 (Output Sensitive Complexity). *When $|\pi_5|$, $|\pi_4|$, and $|\pi_3|$ are all $O(|\pi_1| + |\pi_2|)$, Algorithm Tri Flip Path computes a minimum flip path between two triangulations in time linear in the number of flips it contains.*

Proof. Simply observe that the minimum flip path output by the algorithm contains exactly the flips in π_1 and π_2 . \square

Finally, we prove Theorem 2.

Proof of Theorem 2. For one direction, assume that triangulations U^* and V^* satisfy conditions (i) and (ii) of the theorem. By Theorem 1, the flips in the partial orders π_1 and π_2 in the theorem statement are exactly the flips in the minimum flip plan, constrained by the set of edges E , between these triangulations. Note that the minimum flip plan between any two triangulations U and V , containing sets of edges G and G' respectively, must contain the flips in π_1 and π_2 , because they are defined by the edges in G and G' and do not depend on the triangulations U and V .

For the other direction, without loss of generality, assume that π_1 violates Condition (i), so it contains a flip that is not contained in the minimum flip plan for the edges in G . This flip must be contained in the minimum flip plan π_h , for some other edge h in the triangulation U^* . Furthermore, the root flip in π_h that generates h is contained in π_1 . By Theorem 7, the structure of the flip plan for the edges in U^* allows this root flip to be performed while preserving the edges in G . The minimum flip plan between the resulting triangulation and V^* contains 1 less flip than the minimum flip plan $\pi(U^*, V^*)$.

Next, assume that π_1 satisfies Condition (i), but some flip in π_1 violates Condition (ii). If this flip can be performed in the triangulation V^* , then this yields a triangulation V such that the minimum flip plan between U^* and V contains 1 less flip than the minimum flip plan $\pi(U^*, V^*)$. Otherwise, this flip generates an edge that intersects with an edge h in V^* . The edge h is generated by the minimum flip plan for some edge h' in V^* that is not in G' . This implies that the partial order π_2 violates Condition (i) and we get a similar situation as before. Thus, triangulations U^* and V^* do not attain the minimum in Equation 3. \square

7 Modelling Crack Propagation in Crystalline Materials

The physical phenomenon of crack propagation in crystalline materials caused by Stone-Wales defects can be modelled as the problem of finding a minimum flip path that generates an edge from an equilateral triangulation. Figure 13 shows the hexagonal and tri-hexagonal (also called Kagome) lattices that represent the atoms and bonds of graphene and quartz or 2-dimensional silica respectively, and that underlie other materials such as alumina. The figure also shows how to transform each of these lattices into an equilateral triangulation. For the hexagonal lattice, place a vertex at the center of each hexagon and an edge between pairs of vertices whose hexagons are adjacent. For the tri-hexagonal lattice, modify the previous procedure to place an edge between pairs of vertices whose hexagons share a point. In either case, flips in the triangulation model *Stone-Wales* defects, which occur at the nano-level and cause a bond between atoms to rotate 90 degrees [22].

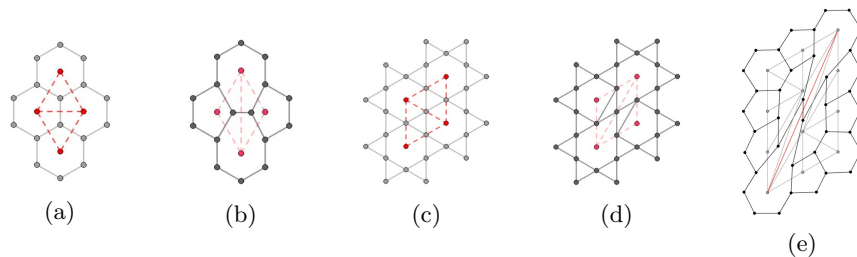


Figure 13: (a) and (b) show how to obtain an equilateral triangulation from the hexagonal lattice (graphene) and the result of one flip (Stone-Wales defect). (c) and (d) show the same for the tri-hexagonal lattice (quartz or 2-dimensional silica). (e) shows a long edge in a triangulation corresponding to a crack in a sheet of graphene caused by a sequence of Stone-Wales defects.

Graphene is susceptible to Stone-Wales defects during synthesis, and when these defects propagate a crack will form at the micro-level [9]. In the context of our model, defect-to-crack propagation corresponds to a minimum flip path that generates a long edge from an equilateral triangulation (Figure 13e). Graphene is being studied for its potential advantages over commonly used materials in electronic devices, such as silicon [14]. When defects appear in a sheet of graphene, its chemical and physical properties are altered. In some cases, Stone-Wales defects are intentionally introduced to tailor a material for a specific application. Techniques have been developed to repair unwanted defects in graphene, such as heating the material or introducing new bonds with different elements. While effective, the mechanics of healing defects are not well understood. Our model elucidates this process.

Currently, material scientists apply finite element analysis techniques to study these defects and the cracks that propagate from them. These tech-

niques involve computational simulations that pin down one side of a sheet of graphene and apply a load perpendicular to that side. It has been observed that when a load is applied in the same direction as a rotated bond, a crack originates at the defect and propagates to form an “X” shape (Figure 10 in [9]). However, these simulations are artificially restricted and computationally expensive. For example, there is no reason why a load cannot be applied in an arbitrary direction on the sheet of graphene. Our model provides a simple and efficient method to generate cracks that does not suffer from the restrictions of a physical simulation.

7.1 A Limitation of Our Model

Consider Figure 14, which depicts the edge $(4, 5)$ in a triangulation and in the corresponding tri-hexagonal lattice. The flips in the flip path for this edge generate edges that are much longer than those in an equilateral triangulation. Since bonds form only between close-by atoms, we must attribute a physical meaning to the long edges. Define a *good* flip to be one that removes an edge contained in an equilateral triangulation and a *bad* flip to be one that removes any other edge. We pose two questions which provide insight into what these edges represent.

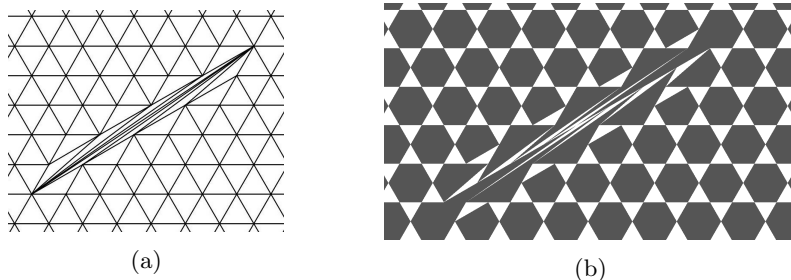


Figure 14: (a) depicts the edge $(4, 5)$ in a triangulation and (b) shows the same edge in the corresponding tri-hexagonal lattice. See Section 7.

Question 1 (Avoiding Bad Flips). *For any edge e , is there a linear ordering of the minimum flip plan that generates the edge e from an equilateral triangulation such that the maximum number of consecutive bad flips is sub-linear in the order of the Farey sequence F_e ?*

Question 2 (Avoiding Long Edges). *Consider an edge e and the triangulation resulting from the minimum flip plan for the edge e . Can the points of this triangulation be perturbed such that the lengths of its edges are small enough to represent bonds between atoms? Note that such a perturbation does not preserve the lattice property. See also Question 3.*

If the answer to Question 1 is positive, then a long, intermediate edge could be related to a measure of the physical load required to break a bond present

in the initial lattice. On the other hand, if the answer to 1 is negative, then Question 2 seeks to determine if we can avoid such edges.

7.2 A Bad Flip Tree

We answer Question 1 in the negative. The starting triangulation of any flip path in this section is an equilateral triangulation.

Theorem 8 (Lower-bound on Bad Flips). *For $n \geq 3$, any linear ordering of the minimum flip plan for the edge $(1, n)$ contains $\Omega(n)$ consecutive bad flips.*

Proof Idea: We will show that the minimum flip plan for the edge $(1, n)$ has height n and that all nodes from heights 3 to n are bad flips. Then, a simple counting argument yields the desired result.

Lemma 11 (Height of Minimum Flip Plan). *The minimum flip plan for the edge $(1, n)$ has height n .*

Proof. We proceed by induction on the size of n . When $n = 1$, the minimum flip plan for the edge $(1, 1)$ has height 1, so the base case is true. Assume the lemma holds for $n = k$ and we will show that it holds for $n = k + 1$. The root of the minimum flip plan for the edge $(1, k + 1)$ is the Farey parallelogram $P_{(1, k+1)}$, and its children are adjacent copies of the Farey parallelogram $P_{(1, k)}$. By Corollary 1 and the inductive hypothesis, the height of DAGs rooted at the child nodes is k . Thus, the height of the minimum flip plan for the edge $(1, k + 1)$ is $k + 1$ and the lemma is proved by induction. \square

For the next lemma, consider an equivalent definition of a flip plan in which each node represents the edge that is flipped in a Farey parallelogram.

Lemma 12 (Mostly Bad Flips). *Consider the minimum flip plan for the edge $(1, n)$, where $n \geq 3$. All nodes at height k , where $3 \leq k \leq n$, are copies of the edge $(1, k - 2)$.*

Proof. We proceed by induction on size of n . When $n = 3$, the minimum flip plan has height 3 by Lemma 11. The root edge $(1, 1)$ is the only node we are interested in, so the base case holds. Assume the lemma holds for $n = j > 3$ and we will show it holds for $n = j + 1$. Again by Lemma 11, the minimum flip plan for the edge $(1, j + 1)$ has height $j + 1$. Consider the Farey parallelogram $P_{(1, j+1)} = \{(0, 1), (1, j)\}$. By Lemma 2, the root node is the edge $(1, j - 1)$ and its children are adjacent copies of the edge $(1, j - 2)$, which is the shorter diagonal of the Farey parallelogram $P_{(1, j)}$. Finally, by Corollary 1 and the inductive hypothesis the DAGs rooted at the child nodes satisfy the lemma. Thus, the lemma is proved by induction. \square

Proof of Theorem 8. By Lemmas 11 and 12, we know that the minimum flip plan for the edge $(1, n)$ has height n and all nodes at heights 3 to n represent bad flips. In the best case, nodes at heights 4 to n will share a distinct child with

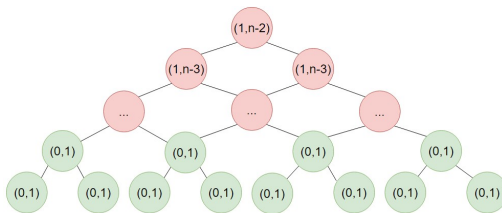


Figure 15: The best case scenario in Theorem 8.

each of its siblings. Also, all nodes at heights 1 or 2 will be good flips and all nodes at heights 1 to 3 will have two unique children. See Figure 15. Counting the nodes at each level then tells us that the minimum flip plan contains at least $\sum_{i=1}^{n-2} i = \Omega(n^2)$ bad flips and at most $4(n-2) = O(n)$ good flips. Thus, if there is a linear ordering of the minimum flip plan for the edge $(1, n)$ that evenly divides the bad flips amongst the good flips, it still contains $\Omega(n)$ consecutive bad flips. \square

7.3 Perturbing Points of the Lattice

There are many embedding techniques that will perturb the points of a triangulation. First, we explore which of these are candidates to answer Question 2. Then, we conjecture which methods can be used to answer a stronger version of the question.

Figure 16 shows an approximate Tutte embedding of the triangulation in Figure 14. The Tutte embedding of a graph is unique [24], meaning that we are stuck with the edge lengths that it gives. As the figure depicts, this method does not eliminate the long edges. The K-A-T embedding of a graph is also unique and fails to suppress these unwanted edges [23].

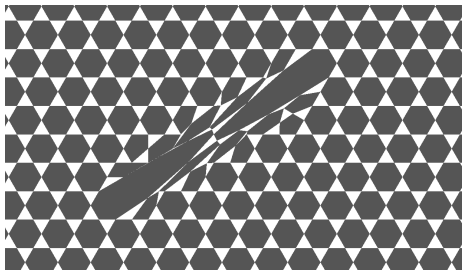


Figure 16: The Tutte embedding of the edge from Figure 14. See Section 7.3.

Two other candidates to inspect are the Delaunay triangulation and almost-equilateral heuristics. The Delaunay triangulation of a point-set is the one that maximizes the minimum angle over all the angles (i.e. it avoids thin triangles) [5]. Given a point-set, the Delaunay triangulation is generally unique; however,

we can reverse the problem and find the set of point-sets for which a triangulation is a Delaunay triangulation. This is a promising path to explore, because we may be able to perturb the points of a triangulation in order to avoid the skinny triangles that arise from generating long edges. Finally, there may be some heuristic that is able to ensure that all edge lengths are bounded by some arbitrary value. This an almost-equilateral embedding. If this method always works for our class of triangulations, then the problem is solved.

Question 2 overlooks the fact that in the physical process of crack propagation the atoms will need to move after each Stone-Wales defect in order to maintain proper bonding distances. We conclude with a stronger version of Question 2, which takes this fact into account, and a conjecture.

Question 3 (Avoiding Long Edges After Each Flip). *Consider an edge e and the sequence of triangulations along the flip path for the edge e . After each flip in the flip path, can the points of the resulting triangulation be perturbed such that the next quadrilateral to be flipped is convex and the lengths of all edges in the triangulation are short enough to represent bonds between atoms?*

Conjecture 1 (Possible Answer to Question 3). *Delaunay triangulations or an almost-equilateral heuristic answer Question 3 in the affirmative.*

8 Conclusion and Further Works

We have elucidated the structure of constrained, minimum flip paths between lattice triangulations, given algorithms with improved complexity over previous algorithms, and given output-sensitive algorithms to compute these paths. Additionally, we have explored an application of our algorithms in modelling crack propagation, as well as discussed the limitations of our model and how to improve it. While the exposition uses closed polygonal regions Ω , this restriction can be removed and we can simply treat the edges of Ω as constraint edges. In fact, all our results can be restated for infinite lattice triangulations that differ by finitely many edges from the infinite equilateral lattice triangulation.

Caputo et al.'s [2] motivation for studying lattice triangulations is to prove bounds for the mixing times of Markov chains over weighted lattice triangulations. This weight allows them to choose whether the Markov chain favor transitions to lattice triangulations containing short edges or to those containing long edges. In both cases, they conjecture mixing time bounds expressed in terms of the dimensions of the point-set, and they prove weak versions of these conjectures. Caputo et al. [2] suggest that a deeper look into the structure of lattice triangulations is necessary to prove the full conjecture. Using structural results about lattice triangulations proved in the current paper, we prove one of these bounds in [21].

Acknowledgments

We thank Maxwell Nolan for computational experiments that led to some of the questions answered in this paper.

References

- [1] Oswin Aichholzer, Wolfgang Mulzer, and Alexander Pilz. Flip distance between triangulations of a simple polygon is np-complete. *Discrete & computational geometry*, 54(2):368–389, 2015.
- [2] Pietro Caputo, Fabio Martinelli, Alistair Sinclair, and Alexandre Stauffer. Random lattice triangulations: Structure and algorithms. *Ann. Appl. Probab.*, 25(3):1650–1685, 6 2015.
- [3] Dimitrios I Dais. Resolving 3-dimensional toric singularities. *Séminaires & Congrès*, 6:155–186, 2002.
- [4] Jesús A De Loera, Jörg Rambau, and Francisco Santos. *Triangulations Structures for algorithms and applications*. Springer, 2010.
- [5] Boris Delaunay et al. Sur la sphere vide. *Izv. Akad. Nauk SSSR, Otdelenie Matematicheskii i Estestvennyka Nauk*, 7(793-800):1–2, 1934.
- [6] AK Dewdney. Wagner’s theorem for torus graphs. *Discrete Mathematics*, 4(2):139–149, 1973.
- [7] Nira Dyn, Ifat Goren, and Shmuel Rippa. Transforming triangulations in polygonal domains. *Computer Aided Geometric Design*, 10(6):531–536, 1993.
- [8] David Eppstein. Happy endings for flip graphs. In *Proceedings of the twenty-third annual symposium on Computational geometry*, pages 92–101, 2007.
- [9] Na Fan, Zhenzhou Ren, Guangyin Jing, Jian Guo, Bei Peng, and Hai Jiang. Numerical investigation of the fracture mechanism of defective graphene sheets. *Materials*, 10(2):164, 2017.
- [10] I Gelfand, M Kapranov, and Andrey V Zelevinsky. Discriminants, resultants and multidimensional determinants. reprint of the 1994 edition. modern birkhäuser classics, 2008.
- [11] Volker Kaibel and Günter M Ziegler. Counting lattice triangulations. *Surveys in combinatorics*, 307:277–307, 2003.
- [12] Johannes F Knauf, Benedikt Krüger, and Klaus Mecke. Entropy of unimodular lattice triangulations. *EPL (Europhysics Letters)*, 109(4):40011, 2015.

- [13] Charles L Lawson. Transforming triangulations. *Discrete mathematics*, 3(4):365–372, 1972.
- [14] Lili Liu, Miaoqing Qing, Yibo Wang, and Shimou Chen. Defects in graphene: generation, healing, and their effects on the properties of graphene: a review. *Journal of Materials Science & Technology*, 31(6):599–606, 2015.
- [15] Atsuhiko Nakamoto and Katsuhiko Ota. Diagonal transformations of graphs and dehn twists of surfaces. *journal of combinatorial theory, Series B*, 70(2):292–300, 1997.
- [16] Seiya Negami. Diagonal flips in triangulations of surfaces. *Discrete Mathematics*, 135(1-3):225–232, 1994.
- [17] Seiya Negami, Shin Watanabe, et al. Diagonal transformations of triangulations on surfaces. *Tsukuba J. Math*, 14:155–166, 1990.
- [18] Eliyahu Osherovich and Alfred M Bruckstein. All triangulations are reachable via sequences of edge-flips: an elementary proof. *Computer Aided Geometric Design*, 25(3):157–161, 2008.
- [19] Mr. J. Farey Sen. Lxxix. on a curious property of vulgar fractions. *The Philosophical Magazine*, 47(217):385–386, 1816.
- [20] William Sims and Meera Sitharam. Flip paths, farey sequences, and material defects. *Pre-print*, 2020.
- [21] William Sims and Meera Sitharam. Mixing time of glauber dynamics over lattice triangulations. *Manuscript*, 2020.
- [22] Anthony J Stone and David J Wales. Theoretical studies of icosahedral c60 and some related species. *Chemical Physics Letters*, 128(5-6):501–503, 1986.
- [23] William P Thurston. *The geometry and topology of three-manifolds*. Princeton University Princeton, NJ, 1979.
- [24] William Thomas Tutte. How to draw a graph. *Proceedings of the London Mathematical Society*, 3(1):743–767, 1963.
- [25] O Ya Viro. Plane real algebraic curves: constructions with controlled topology. *Algebra i analiz*, 1:1–73, 1989.
- [26] Klaus Wagner. Bemerkungen zum vierfarbenproblem. *Jahresbericht der Deutschen Mathematiker-Vereinigung*, 46:26–32, 1936.